ISSN 2070-0482, Mathematical Models and Computer Simulations, 2015, Vol. 7, No. 4, pp. 339–348. © Pleiades Publishing, Ltd., 2015.
Original Russian Text © Yu.I. Shokin, S.A. Beisel, A.D. Rychkov, L.B. Chubarov, 2015, published in Matematicheskoe Modelirovanie, 2015, Vol. 27, No. 1, pp. 99–112.

Numerical Simulation of the Tsunami Run-Up on the Coast Using the Method of Large Particles

Yu. I. Shokin, S. A. Beisel, A. D. Rychkov, and L. B. Chubarov

Institute of Computational Technologies, Siberian Branch, Russian Academy of Sciences, Novosibirsk, Russia
Novosibirsk State University, Novosibirsk, Russia
e-mail: chubarov@ict.nsc.ru

Received January 28, 2014

Abstract—An approach to the computer simulation of a tsunami run-up on the coast is presented, based on nested grids and the large-particle method. The computational algorithms are based on the classical equations of shallow-water theory. The main elements of the developed computational technology are described and the results are given of the verification and validation of numerical algorithms, as well as the mathematical model and of one- and two-dimensional test problems. The capabilities of the algorithms developed by the authors are demonstrated for the calculation of the defining parameters of the tsunami run-up on the coast in the vicinity of the town of Severo-Kurilsk (November 5, 1952).

Keywords: mathematical modeling, tsunami waves, run-up, method of large particles

DOI: 10.1134/S2070048215040109

1. INTRODUCTION

In solving practical problems of tsunami hazard mitigation, detailed information about the expected range and depth of the coastal flooding zone, as well as an evaluation of the current velocities in this area, are of paramount importance. The availability of this information allows one to determine the size of evacuation zones and evaluate the possible economic damage caused by this natural phenomenon. The assessment of the run-up parameters even for the known wave height at the water's edge (or at some fixed depth) is a complex problem, which requires special computation methods that are different from those used for the simulation of tsunami propagation in deep water.

It is well known that for a complex and rugged coastline, the height and distance of a run-up on a shore crucially depend not only on the height of the tsunami wave approaching the shallow waters but also on its length (period), as well as on the direction of approach to a specific cove or bay. An example of such a relationship is the height of the run-up on the coast of Sanriku measured after the devastating Tohoku tsunami on March 11, 2011 [1]. Instrumental recordings made by bottom sensors installed at intermediate depths [2] show that in the coastal area, which lies directly opposite the earthquake focus, the height of the approaching tsunami wave was 5–7 m and was about the same for nearly 300 miles along the front, changing by not more than 30–40%. This is also confirmed by the analysis of the run-up heights measured on headlands projecting into the sea, which over a large area along the coast were also about the same and were equal to 10–12 meters. At the same time, the run-up heights measured in the gulfs and at bayheads varied in a much wider range from ten to forty meters; i.e., their variation range exceeds 400%. Equally significant were the variations in the flooding depth for the areas adjacent to the bays and coves. This confirms the importance of correctly assessing the characteristics of the wave run-up on a shore for specific coast segments and the significance of studying the variations of these characteristics in bays and coves at different parameters and locations of tsunami sources.

There are many numerical methods developed for the solution of the above-mentioned problems of wave hydrodynamics. Recently, the gridless SPH (Smoothed Particle Hydrodynamics) method [3], which is a further development of the technique referred to as particle-in-cell (PIC), has become popular. There is no Euler stage in SPH, which, on the one hand, made this method more robust and applicable to calculations of flows in complex domains but, on the other hand, its use requires the development of complex smoothing procedures describing interactions between particles, which undermines the conservatism of the method. In the method of large particles [4] (LP), which in our work is applied to the problem on the dynamics of tsunami waves within the shallow water theory, as in SPH technique, we use particles in the form of an "elementary water column" (fluid element), further referred to as "large particles" whose

motion is described in two stages, i.e., the Lagrangian and Eulerian stages, which significantly simplifies the procedure for accounting for the interaction of particles and at the same time provides a sufficiently accurate reconstruction of the wave run-up (backwash) on a coast and strict adherence to the laws of conservation. It should be noted that in order to attain the necessary accuracy for the solution of two-dimensional problems by the SPH method, about 100000 particles is required [5]. This is comparable to the number of difference grid nodes in the LP method; however, the software implementation of the LP technique is much simpler and the number of operations required for the calculation of the motion of a single large particle is approximately two orders of magnitude less than for the SPH method.

The proposed method for the calculation of the tsunami run-up on a coast combines the use of the large-particle method in the littoral zone and the MacCormack scheme for calculating the propagation of tsunamis in deep water. We employed nested grids, which made it possible to develop an algorithm implemented as a complex of programs, which has been used to determine the characteristics of the tsunami run-up from a model earthquake near Severo-Kurilsk in the Russian Far East.

The results of the algorithm verification and model validation on the test problems suggest that the proposed and thoroughly proven methodology will also work well in solving problems which involve practical calculations of a run-up on a real heavily indented coastline and the corresponding configuration of the littoral zone.

2. MODELS AND ALGORITHMS FOR CALCULATING THE CHARACTERISTICS OF A TSUNAMI RUN-UP ON A LITTORAL ZONE

For solving problems of a tsunami run-up on the coast the authors selected a well-known mathematical model of shallow water, taking into account the friction force averaged over the depth and the Coriolis force. The corresponding equations are written in a spherical coordinate system in which the surface $r = R_E$ coincides with the undisturbed free surface

$$\begin{gathered}\frac{\partial H}{\partial t}+\frac{1}{R_E\cos(\phi)}\left[\frac{\partial(Hu_\lambda)}{\partial\lambda}+\frac{\partial(H\cos(\phi)u_\phi)}{\partial\phi}\right]=0,\\ \frac{\partial u_\lambda}{\partial t}+\frac{1}{R_E}\left[\frac{1}{2\cos(\phi)}\frac{\partial(u_\lambda^2)}{\partial\lambda}+u_\phi\frac{\partial u_\lambda}{\partial\phi}+\frac{g}{\cos(\phi)}\frac{\partial(H-h)}{\partial\lambda}\right]=f_\lambda,\\ \frac{\partial u_\phi}{\partial t}+\frac{1}{R_E}\left[\frac{u_\lambda}{\cos(\phi)}\frac{\partial u_\phi}{\partial\lambda}+\frac{1}{2}\frac{\partial(u_\phi^2)}{\partial\phi}+g\frac{\partial(H-h)}{\partial\phi}\right]=f_\phi,\end{gathered}\qquad(1)$$

where $H(\lambda,\phi,t)$ and $h(\lambda,\phi)$ are the total depth of water and the bottom profile measured from the surface of the "quiet" water, respectively, $u_\lambda(\lambda,\phi,t)$, $u_\phi(\lambda,\phi,t)$ are the depth-averaged components of the velocity vector in directions λ and ϕ, respectively, $f_\lambda=\alpha u_\phi-gk_f^2u_\lambda\sqrt{u_\lambda^2+u_\phi^2}\big/H^{4/3}$, $f_\phi=-\alpha u_\lambda-gk_f^2u_\phi\sqrt{u_\lambda^2+u_\phi^2}\big/H^{4/3}$, $\alpha=2\omega_E\sin(\phi)$, and k_f is the roughness coefficient (Chezy friction coefficient). The mean radius of the Earth R_E is taken to be 6371 km and the Earth's angular velocity $\omega_E=7.292115\times10^{-5}\,1/\mathrm{s}$.

In system (1), in order to avoid division by zero, the possible variation range of coordinate ϕ is determined as follows: $-\frac{17\pi}{36}\le\phi\le\frac{17\pi}{36}$. Since the motion of the fluid within the planetary scale is bounded on the South Pole by the Antarctic, and on the north scale it is bounded by the polar ice caps, the specified limit on the change in the coordinate ϕ is quite reasonable, and does not limit the application of the system of equations for the description of wave propagation on the Earth's surface.

In order to simulate the processes of tsunami generation, propagation, and the run-up on the real coast within the shallow-water theory, we developed a software system which numerically implements these processes on nested difference grids related to global and small domains. The global domain is understood here as a rectangular area covering part of the coast and the oceanic zone in which the tsunami wave is generated and propagates to the coast. The small domain is a subdomain of the global domain, including part of the dry land and ocean area, whose borders are crossed by a tsunami wave during its motion to the coast, whose run-up we are to calculate. At the same time, the wave propagation in the global domain is simulated on a coarser grid (although it is sufficiently fine to yield adequate results) and in the small subdomain we use a grid with a smaller space step required for a detailed computation of the wave run-up characteristics. In the global domain, the run-up is not calculated, and along the initial shoreline, we impose a condition of reflection ("vertical wall"). In order to prevent the effect of "drying" in the simu-

lation of wave interaction with the shore represented by such a wall, depths, which are less than a certain threshold value ($0 < h < h_{\min}$), are replaced by $h_{\min}$.

The calculation on nested grids is based on a standard technique where a perturbation is transferred from a global domain to a small subdomain using the values of parameters in the coarse grid nodes along the external maritime borders of the small subdomain. In order to convert these boundary values from the coarse grid to a refined one we use a linear interpolation both in space and in time (when the current time step of the fine grid is less than the time step of the coarser grid).

Thus, the solution algorithm consists of two main stages. At the first stage, on the main (coarse grid) at each new $(n + 1)$th time step in the global domain we find the solution of the wave propagation problem which is interpolated to the fine grid on the boundaries of the small domain. Using these values, we calculate the interaction between the waves and the coast in the small domain, after which the obtained new wave fields (total depth, velocities) are interpolated to the coarse grid, thereby providing the feedback effect of the solution in the small domain on the solution in the global domain.

The initial moment of the run-up calculation may fail to coincide with the starting point for the propagation computation. This is used for reducing the calculation time when the initial displacement of the water surface is fairly remote from the "protected" segment of the coast and the wave process is not manifested in the small subdomain for some time. The moment of the wave's approach to the small subdomain and, accordingly, the initial instant of the wave run-up calculation is determined during the preliminary calculations of the wave's propagation from the model source in the global domain on the coarse grid. Here, the coast segments referred to as "protected" are those in which settlements or economic entities are located for which the damage potentially inflicted by tsunami is to be minimized.

A detailed description of mathematical models and algorithms used by the authors for the numerical simulation of the generation and propagation of tsunami waves in the global domain (up to the initial position of the shoreline), as well as for the test calculations, are presented in [6]. Here we will only point out that the process of tsunami wave generation by underwater earthquakes is reconstructed within the "piston" model with a dislocation source of the earthquake [7] and the numerical algorithm for the calculation of the wave propagation in the global domain is based on the finite-difference second order MacCormack scheme [8].

A tsunami wave run-up on the coast within the "small" domain is simulated by the large-particle method [4]. The use of the classical particle-in-cell method for solving this class of problems is impossible due to the statistical nature of its resulting solution, which, in particular, does not satisfy the condition of hydrostatic equilibrium in the water at rest and significantly distorts the process of wave propagation. The large-particle method is free from this drawback and allows one to obtain a balanced difference scheme. It is implemented on a uniform rectangular difference grid for the following reasons:

• the actual coast, as a rule, is heavily indented, and therefore it is difficult to build a curved difference grid suitable for the solution of (1);

• during the wave run-up, some water penetrates into depressions formed by the land topography (river estuaries, canyons, etc.) and flows past various mounds; therefore, it does not seem feasible to use an adaptive grid tied to the coastline.

The large-particle method is implemented in two stages. At the first (Euler) stage, all convective terms in system (1) are discarded and the system is written as

$$\begin{gathered}\frac{\partial H}{\partial t} = 0,\\ \frac{\partial u_\lambda}{\partial t} + \frac{g}{R_E \cos(\phi)}\frac{\partial (H-h)}{\partial \lambda} = -u_\lambda C_R + \alpha u_\phi,\\ \frac{\partial u_\phi}{\partial t} + \frac{g}{R_E}\frac{\partial (H-h)}{\partial \phi} = -u_\phi C_R - \alpha u_\lambda,\end{gathered} \tag{2}$$

where $C_R = g k_f^2 \dfrac{\sqrt{u_\lambda^2 + u_\phi^2}}{H^{4/3}}$.

At the second (Lagrangian) stage, we solve the transport equations

$$\frac{\partial H}{\partial t}+\frac{1}{R_E\cos(\phi)}\left[\frac{\partial(Hu_\lambda)}{\partial\lambda}+\frac{\partial(H\cos(\phi)u_\phi)}{\partial\phi}\right]=0,$$
$$\frac{\partial u_\lambda}{\partial t}+\frac{1}{R_E}\left[\frac{1}{2\cos(\phi)}\frac{\partial(u_\lambda^2)}{\partial\lambda}+u_\phi\frac{\partial u_\lambda}{\partial\phi}\right]=0, \quad (3)$$
$$\frac{\partial u_\phi}{\partial t}+\frac{1}{R_E}\left[\frac{u_\lambda}{\cos(\phi)}\frac{\partial u_\phi}{\partial\lambda}+\frac{1}{2}\frac{\partial(u_\phi^2)}{\partial\phi}\right]=0.$$

Equations (2) and (3) are solved by constructing an explicit difference scheme of the first-order accuracy on a staggered pattern for the grid values of free surface depths and elevations to be determined in the grid nodes and the velocity values to be obtained in the middle of the respective edges. We note that since the coast topography is highly jagged, in order to obtain a numerical solution with an adequate resolution of the picture of the tsunami's run-up on the shore, as already mentioned, the difference grid must be sufficiently detailed. Therefore, it appears justified to employ a scheme with first-order accuracy and monotonic properties.

The difference scheme of the first stage is written as follows:

$$\tilde H_{i,j}=H^n_{i,j},$$
$$\tilde u_{\lambda,i+1/2,j}=(u^n_{\lambda,i+1/2,j}-g\Delta t((H-h)^n_{i+1,j}-(H-h)^n_{i,j})/(R_E\cos(\phi_j)\Delta\lambda)+\Delta t\alpha u_\phi)/(1+\Delta tC_R),$$
$$\tilde u_{\phi,i,j+1/2}=(u^n_{\phi,i,j+1/2}-g\Delta t((H-h)^n_{i,j+1}-(H-h)^n_{i,j})/(R_E\Delta\phi)-\Delta t\alpha u_\lambda)/(1+\Delta tC_R).$$

At the second stage, for the transport equations (3), an upwind difference scheme is used

$$H^{n+1}_{i,j}=\tilde H_{i,j}-\Delta t((\tilde q_{i+1/2,j}-\tilde q_{i-1/2,j})/\Delta x+(\tilde q_{i,j+1/2}-\tilde q_{i,j-1/2})/\Delta y),$$
$$\tilde q_{i+1/2,j}=\begin{Bmatrix}\tilde H_{i,j}\tilde u_{\lambda,i+1/2,j}\ \text{if}\ \tilde u_{\lambda,i+1/2,j}>0,\\ \tilde H_{i+1,j}\tilde u_{\lambda,i+1/2,j}\ \text{if}\ \tilde u_{\lambda,i+1/2,j}<0\end{Bmatrix}, \quad (4)$$
$$\tilde q_{i,j+1/2}=\begin{Bmatrix}\tilde H_{i,j}\tilde u_{\phi,i,j+1/2}\ \text{if}\ \tilde u_{\phi,i,j+1/2}>0,\\ \tilde H_{i,j+1}u_{\phi,i,j+1/2}\ \text{if}\ \tilde u_{\phi,i,j+1/2}<0\end{Bmatrix}.$$

Similarly we can write expressions for the calculations of the values $(u_\lambda)^{n+1}_{i+1/2,j}$ and $(u_\phi)^{n+1}_{i,j+1/2}$. The condition for the stability of the difference scheme is the fulfillment of the inequality $\Delta t\le\alpha\cdot\min\left\{\frac{\Delta x}{|u_\lambda|+\sqrt{gH}},\frac{\Delta y}{|u_\phi|+\sqrt{gH}}\right\}$ in all nodes of the difference scheme where $0<\alpha<1$ is the empirical stability factor, which for the computational experiments presented below was taken within the range 0.4–0.7.

The water's edge was determined by capturing it in the difference grid node; in this technique for calculating the flow parameters at each time step the grid nodes are identified, in which the total depth H does not exceed some small parameter, which in the calculations below was taken equal to 10^{-3}. These nodes are assumed to be dry and all flow parameters in them are assumed to be zero, including the free surface deviation from the undisturbed level $\eta=H-h$. In the grid nodes on the boundary of the water and land, the system of shallow water equations is written in the nondivergent form and at the Euler stage for the calculation of velocities u_λ and u_ϕ derivatives $\frac{\partial(H-h)}{\partial\lambda}$ and $\frac{\partial(H-h)}{\partial\phi}$ are approximated by one-sided differences (see (4)). Thus, the moving border between the water and land (water edge) is determined with an accuracy up to the grid step size and appears as a stepwise curve on the employed rectangular grid.

The application software for the run-up calculation has been implemented as a separate module [9] embedded in the MGC [10] earlier developed by the authors. This module allows the calculation of the following characteristics of the interaction between tsunami waves and the protected coast in the small domain:

* intermediate free surfaces at the user-selected time points (with an equal interval);

* intermediate fields of each velocity components at the same time points;

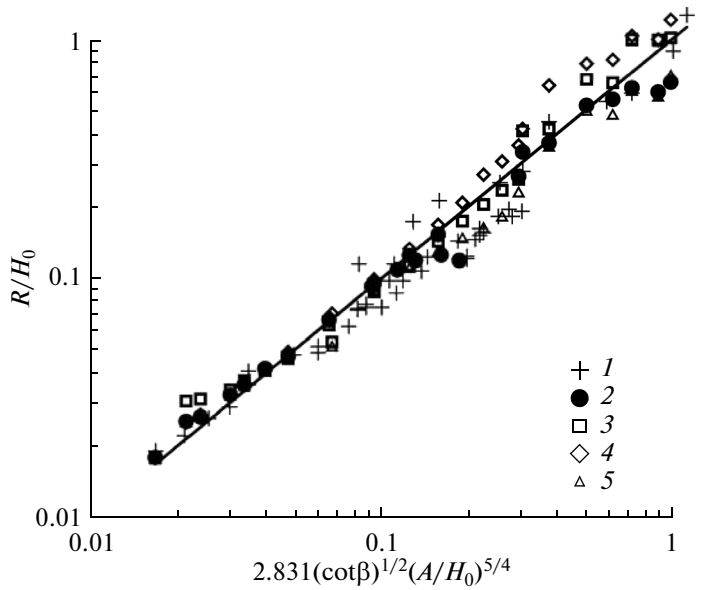

Fig. 1. Problem of a solitary wave run-up on a plane beach. The values of the maximum run-ups obtained by the analytical formula (solid line), by laboratory experiments (*1*), and by numerical large-particle methods (*2*), shock-capturing method (*3*), method of adaptive grids (*4*), and finite-difference method based on the modified model of shallow water (*5*).

* "glow" patterns—arrays of the maximum and minimum values of the free surface at each node of the fine grid over the entire time of the run-up calculation;

* arrays of the maximum depths of the coast flooding at each node of the fine grid over the entire time of the run-up calculation;

* arrays of the maximum values of the wave velocity module at each node of the fine grid over the entire time of the run-up calculation;

* duration of the coast flooding calculated as the total time, during which the originally "dry" grid nodes were flooded during the wave run-up;

* masks (templates) of the coast flooding and bottom dewatering zones, i.e., arrays, in which every grid node by being assigned some integer value is assigned to one of four types, i.e.: a node initially "dry" and remaining "dry" (not flooded over the entire run-up time) during the entire calculation time; initially "dry" but flooded during the run-up; initially "wet" (covered with water) but exposed during drying (wave backwash); initially "wet" and remaining "wet" (not exposed during drying) during the entire calculation time.

3. VERIFICATION OF THE NUMERICAL ALGORITHM AND VALIDATION OF THE MATHEMATICAL MODEL

Numerical methods for the calculation of a wave run-up on shore were verified on well-known test problems [11] in one-dimensional and two-dimensional statements.

In the one-dimensional case, we considered a problem of a solitary wave run-up on a plane beach with an angle β linked with a section of the flat bottom at depth H_0. The corresponding initial displacement of the free surface and velocity field were given by the formulas

$$\eta(x,0)=\frac{A}{\cosh^2(Z)},\quad Z=\sqrt{\frac{3A}{4(H_0+A)}}\cdot\frac{(x-x_0)}{H_0},\quad u(x,0)=-\frac{\eta\sqrt{g(H_0+A)}}{H_0+\eta},$$

where A is the amplitude of the solitary wave and x_0 is the initial position of its crest.

The following analytical solution for the determination of the vertical run-up for the considered problem was obtained in [12]:

$$R/H_0=2.831\sqrt{\cot\beta}\,(A/H_0)^{5/4}. \tag{5}$$

This formula is applicable within $(0.288\tan\beta)^2 \ll A/H_0 < 0.479(\tan\beta)^{10/9}$.

In order to verify the numerical algorithm we used the following values of parameters characterizing the problem statement: for the angle of the slope with $\cot\beta = 19.85$ waves with the relative amplitude A/H_0 were considered in the range from 0.005 to 0.05 with step 0.005; for waves with $A/H_0 = 0.01$ the slope angle β was used for 1, 2, 4, 5, 8, and 10 degrees; for slope angles of 10 and 15 degrees waves with the relative amplitude of 0.1, 0.15, and 0.2 were taken.

Figure 1 shows a comparison between the values of a vertical run-up which were obtained by the analytical formula (5) and those calculated by the large-particle method. In addition, we present the results of laboratory experiments [12, 13] and of calculations using other numerical algorithms, i.e., the shock-capturing method [14], the method of adaptive grids using an approximate analytical expression similar to the condition imposed on the problem of the gas flow into the vacuum [15] as a boundary condition on a moving shore edge, and the finite-difference method based on a modified shallow-water model [16].

A series of computational experiments was also carried out in a two-dimensional statement and the results obtained by the authors were compared with field data [17] performed in a rectangular research basin with width $L_y = 30$ m and length $L_x = 25$ m; the depth of the undisturbed water layer $H_0 = 0.32$ m. In the central part of the basin, there was an island shaped as a right circular cone with a radius of the lower base $R_0 = 3.6$ m and the radius of the upper base $R_1 = 1.1$ m. The height of the cone $H_1 = 0.625$ m; i.e., the tilt angle of the cone generator at the base was $\beta \approx 14^\circ$ ($\tan\beta = 1/4$).The side walls of the basin were made of a special material that absorbed the approaching waves (with the minimum reflection).

The solitary wave entering the basin in the laboratory experiment was generated by the controlled movement of a wave-maker, $A_0 = 0.015$, 0.03, 0.06 m (experiments *A*, *B*, *C*, respectively).

The problem of the computational experiment was set in the right-hand coordinate system, in which axis *Oy* was directed parallel to the wave generator and *Ox* was perpendicular to it towards the island. It was also assumed that the origin of the coordinate system coincided with the edge of the wave generator and the center of the model island was located at the point with coordinates $x_0 = 12.96$ m and $y_0 = 13.80$ m.

In the set-up of the computational experiment, the problem was slightly simplified with respect to the solitary wave incident on the island; i.e., the simulated motion of the wave generator was replaced by a solitary wave (soliton) with amplitude A_0 entering through the boundary

$$\eta(0,y,t) = A_0\operatorname{sech}^2\left\{\left(\frac{3A_0}{4H_0^2(H_0+A_0)}\right)^{1/2}(x_0 - ct)\right\}, \quad c = \sqrt{g(H_0+A_0)}.$$

At the interior points closest to the input boundary, a normal component of velocity u_n was set, calculated by the formula $u_n = c\eta/(h+\eta)$. The tangential component of velocity v in the internal nodes of the grid adjacent to the front edge was calculated from the ratio $u_y = v_x$, which results from the assumption of a quasi-potential velocity vector **u**. This relation is exactly satisfied in the parts of the basin where the depth is constant. On the other boundaries, the well-known "absorbing" Sommerfeld conditions were set, given by the equation $f_t + cf_n = 0$, where direction *n* coincides with the direction of the outward normal to the boundary. The results presented below correspond to experiments (*A*) – $A_0^A = 0.015$ m and (*B*) – $A_0^B = 0.03$ m. In this case, a uniform difference grid was used with the step of 2 cm.

It turned out that the general character of the wave process only slightly depends on the initial amplitude A_0 (experiments *A*, *B*): the solitary wave with the amplitude increasing in the course of its interaction with the model island wraps around it and forms in the rear part of the island a zone of energy concentration, which moves toward the output boundary. This wave formation is followed by a succession of concentric waves, which leave the basin through lateral outlet boundaries. The time-successive states of the free surface shown below in Fig. 2 were calculated for experiment (*A*) without allowance for the bottom friction.

As shown by the results below, the calculated values are in good qualitative and quantitative agreement with the field data and, in particular, adequately reproduce the change of the vertical run-up when the wave flows around the island; i.e., the maximum run-up is observed on the front side, then while flowing around the island it gradually decreases, and on the rear side, there is another extremum of the run-up value.

The run-up height distribution along the perimeter of the conical island (Fig. 3) calculated during the test trials for different values of the roughness parameter (k_f) shows a tendency to form a shadow ("safe")

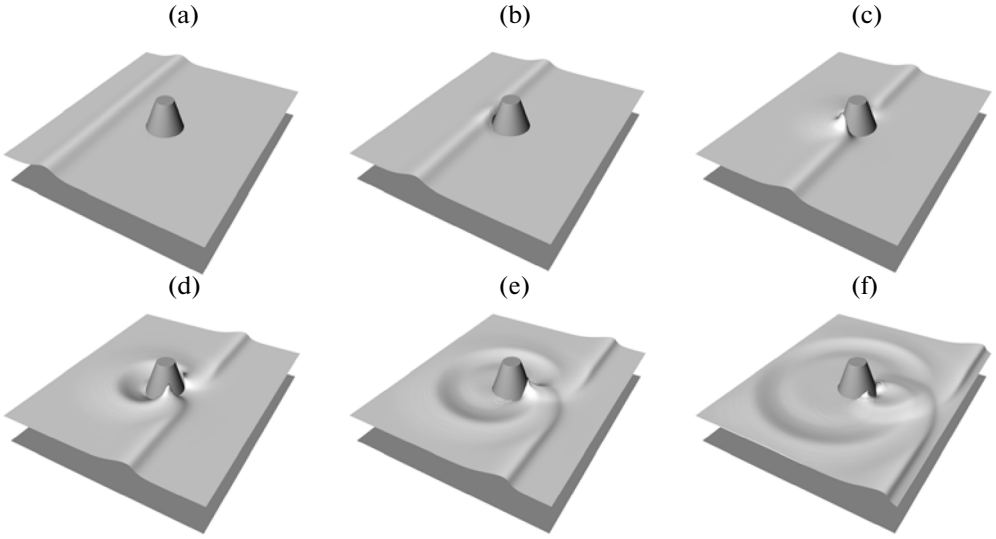

Fig. 2. Time-successive states of the free surface at the interaction of a solitary wave with a conical island. The vertical scale of the free surface is by a factor of 6 higher than the vertical scale of the bottom.

zone at the approach to the back side of the island and a significant increase in the height of the run-up in its rearmost part.

The results presented in the figure clearly indicate that the studied process is nonlinear. This is manifested in the fact that while for the small amplitude of the incident wave (experiment *A*) it is possible to select the roughness parameter (Chezy friction coefficient), at which the results of the numerical simulation are close to the experimental data along the entire perimeter of the conical island, no such uniform parameter can be fitted when the incident wave amplitude increases (experiment *B*). In this case, the experimental data in the run-up in the rear zone can be adequately reproduced at the zero Chezy friction coefficient, and in the remaining part, they can be reproduced at its value of 0.004. It should also be noted that the increase in the amplitude of the incident wave is also accompanied by a growing difference between the results obtained for different friction coefficients.

The comparison of the numerical results with the measured data shows that, despite the simplification in setting the initial perturbation, the mathematical model and computational algorithm based on it adequately reproduce the process of solitary wave interaction with an obstacle in the form of a conical island. The results also demonstrate the convergence to the experimental data when the properties (roughness) of the flooded land are properly selected.

Thus, the results of the model and algorithm testing show that the developed computational tools are quite adequate for the simulation of tsunami waves as a whole, from their generation up to their run-up on the coast. The same findings, however, prove that accuracy ensuring the acceptable reliability of the predictive estimate of parameters characterizing the interaction of tsunami waves with the coast can only be obtained based on detailed numerical information (with a digitizing step of about 15 m) on the bathymetry of water areas adjacent to protected coastal zones and the characteristics of land topography (vegetation, parameters of the Earth's surface, the presence of buildings and their characteristics, etc.).

4. EXAMPLE OF MODELING A TSUNAMI RUN-UP ON THE COAST

As an example of the simulated interaction of tsunami waves with a real coast, we present the numerically calculated characteristics of the run-up of tsunami waves generated by one of the strongest earthquakes recorded in the Kuril-Kamchatka region, which took place on November 5, 1952 (its magnitude according to various estimates was $M_W = 8.4–9.0$) on the coast adjacent to the town of Severo-Kurilsk. The epicenter of this earthquake was located at coordinates 159.5° E, 52.75° N, and the run-up heights in Severo-Kurilsk were up to 15–18 m.

For modeling tsunami generation and wave propagation from the source region to the coast, a global domain was selected extending from east to west from 154.3° E to 164.0° E; and from the south to the north, 48.7° N to 55.0° N. The corresponding borders of the small domain for the run-up simulation ranged from 156.1° E to 156.3° E and from 50.6° N to 50.725° N.

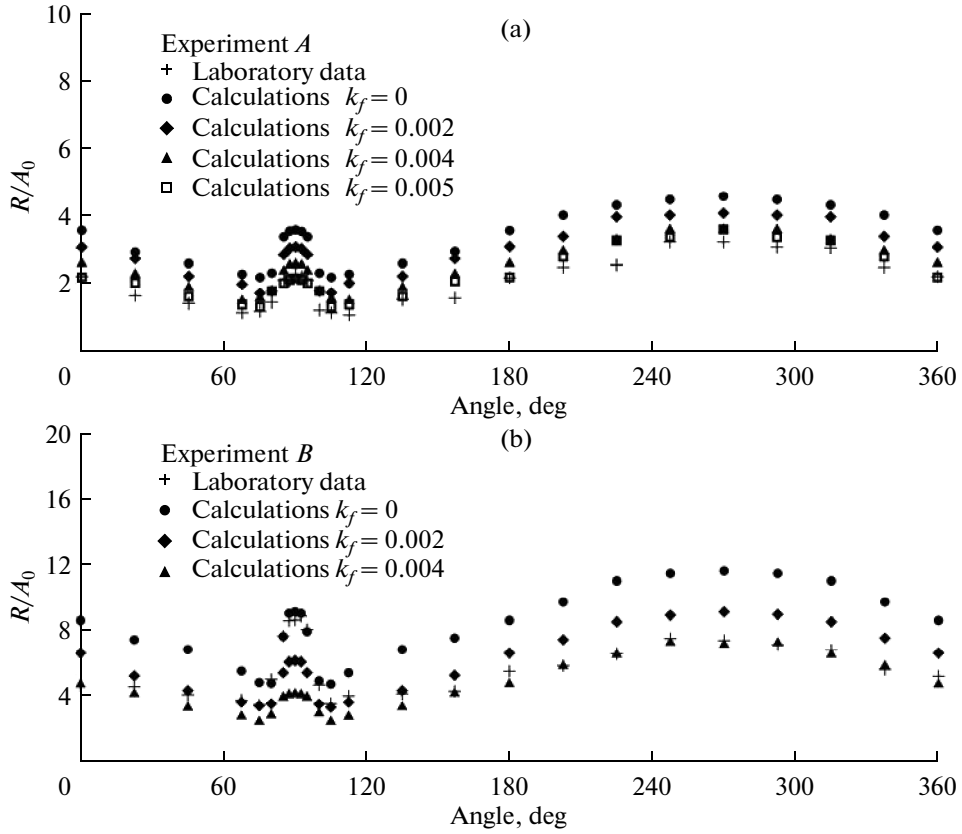

Fig. 3. Distributions of the run-up heights of a solitary wave along the perimeter of the conical island for experiments *A* (a) and *B* (b) calculated for different values of the roughness coefficient versus the experimental data. Along the horizontal axis there is a plotted value of the central angle varying clockwise so that the value 270° corresponds to the direction of the wave approach (front part of the island); and 90°, to the rear part of the island.

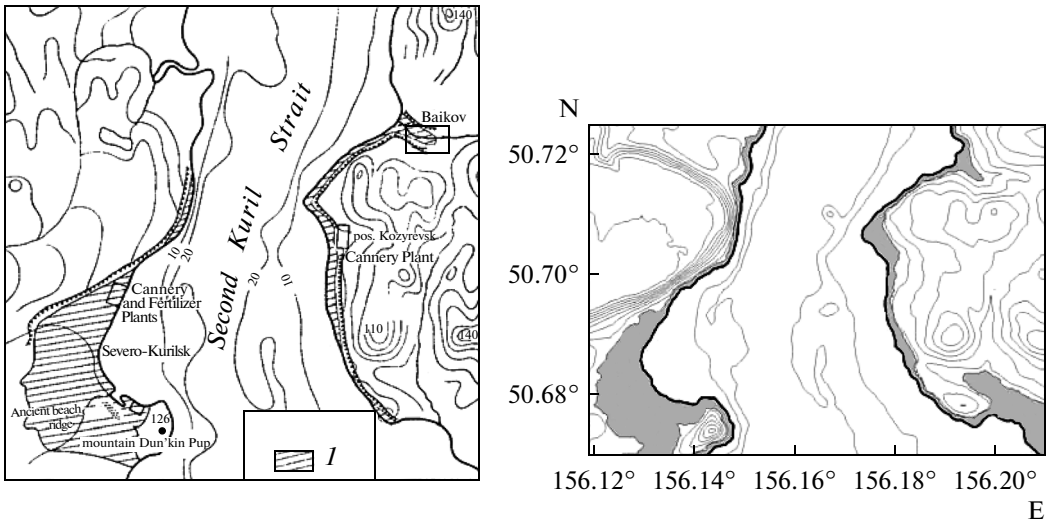

Fig. 4. Comparison of flooded areas (shaded areas) in the second Kuril Strait in the vicinity of Severo-Kurilsk: field data on the tsunami of November 5, 1952 [21] (left) and numerical results (right).

As a bathymetric array for the global domain, we used a fragment of a digital array GEBCO-30sec [18] reinterpolated to the grid with a step of 10 arcseconds. Detailed digital arrays of the topography and bathymetry in the small domain had a spatial step of 1 arcsecond (about 30 meters). Here, the source of

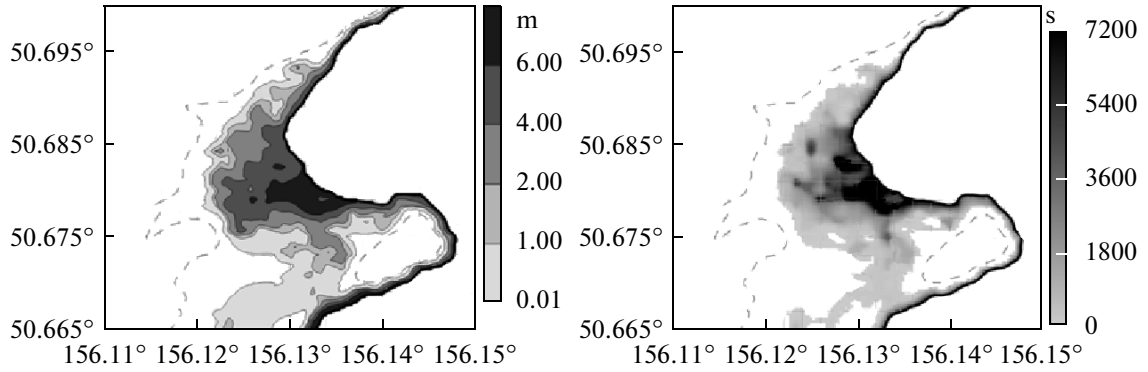

Fig. 5. Distribution of maximum depths (left) and duration of flooding more than 0.1 m deep (right) in the vicinity of Severo-Kurilsk obtained by the computational experiments. The dashed line shows the isoline of the land relief of 20 m.

information for the construction of a digital image of the land topography was array SRTM-3sec (SRTM version 2.1 [19]). The bathymetry array of water areas adjacent to the protected zones of the coast was constructed using images from publicly available bathymetric [20] and navigational charts digitized by the authors.

As a model source, a hypothetical seismic source was considered with magnitude $M_W = 8.8$, the length of the rupture was 300 km, the width was 120 km, the incidence angle of the seismic fault was 45° (dip angle), the direction of the shift in the seismic fault plane was 90° (rake angle), the azimuth of the strike shift was 35°, the depth of the upper edge of the fault was 10 km, and the shift was 10 m.

In order to assess the adequacy of numerical simulation of the tsunami run-up, we present a comparison of the calculated and recorded run-up zone in the neighborhood of Severo-Kurilsk (Fig. 4). There is good agreement between the historical data on the boundaries of the flooded coastal zone [22] and the computation results where the run-up heights also almost reached 20 m.

Figure 5 shows the distribution of the calculated maximum depths (left) and duration of flooding with depths exceeding 0.1 m (right) in the vicinity of Severo-Kurilsk. As can be seen from the figure, the depths of coastal flooding obtained by the computational experiments are up to six meters and more and the flooding duration can be up to several hours.

ACKNOWLEDGMENTS

This work was supported by the Russian Foundation for Basic Research, project no. 12-05-00894; Program for Integrated Basic Research of the Siberian Branch of the Russian Academy of Sciences, projects no. 117A, 37B; Program of the Presidium of Russian Academy of Sciences, project no. 4.10; and the Presidential program "Leading Scientific Schools of the Russian Federation," project no NS-5006.2014.9.

REFERENCES

1. N. Mori, T. Takahashi, and The 2011 Tohoku Earthquake Tsunami Joint Survey Group, "Nationwide post event survey and analysis of the 2011 Tohoku earthquake tsunami," Coast. Eng. J. **54**, 1–27 (2012).
2. H. Kawai, M. Sato, K. Kawaguchi, and K. Seki, "The 2011 off the Pacific coast of Tohoku earthquake tsunami observed by GPS buoys," J. Jpn. Soc. Civil Eng., Ser. B2 **67**, 1291–1295 (2011).
3. G. Oger, M. Doring, B. Alessandrini, and P. Ferrant, "Two-dimensional SPH simulations of wedge water entries," J. Comput. Phys. **213**, 803–822 (2006).
4. O. M. Belotserkovskii and Yu. M. Davydov, *Large Particle Method in Gasdynamics* (Nauka, Moscow, 1982) [in Russian].
5. M. de Leffe, D. le Touze, and B. Alessandrini, "SPH modeling of shallow-water coastal flows," J. Hydraul. Res. **48** (extra iss.), 118–125 (2010).
6. V. S. Kosykh, L. B. Chubarov, V. K. Gusyakov, D. A. Kamaev, V. M. Grigor'eva, and S. A. Beisel, "Methods for calculating the maximum height of the tsunami waves in the protected areas of the Far East coast of the Russian Federation," Inform. Sbornik: Rezult. Ispyt. Nov. Usovershenst. Tekhnol. Modelei Metodov Gidrometeorol. Prognozov, No. 40, 115–134 (2013).

7. V. K. Gusiakov, "Residual displacements on the surface of elastic half-space," in *Conditionally Correct Problems of Mathematical Physics in Interpretation of Geophysical Observations* (Vychisl. Tsentr Sib. Otdel. RAN, Novosibirsk, 1978), pp. 23–51 [in Russian].
8. R. W. MacCormack, "The effect of viscosity in hypervelocity impact cratering," J. Spacecraft Rockets **40**, 757–763, 2003.
9. A. D. Rychkov, S. A. Beisel, and L. B. Chubarov, "Computer Program: Module for calculation of runup of tsunami waves on a coast RunUp-LP," State Registration Certificate of Computer Program No. 2013617980.
10. L. B. Chubarov, V. V. Babailov, and S. A. Beisel, "Program for calculating parameters of seismogenetic tsunami waves MGC," State Registration Certificate of Computer Program No. 2011614598.
11. *Long-Wave Runup Models*, Ed. by H. Yeh, P. Liu, and C. E. Synolakis (World Scientific, Singapore, 1996).
12. C. E. Synolakis, "The runup of solitary waves," J. Fluid Mech. **185**, 523–545 (1987).
13. C. E. Synolakis, "Tsunami runup on steep slopes: how good linear theory really is," Natural Hazards **4**, 221–234 (1991).
14. Z. I. Fedotova, "Numerical method validation for modeling of long waves runup on a coast," Vychisl. Tekhnol. **7** (5), 58–76 (2002).
15. S. P. Bautin, S. L. Deryabin, A. F. Sommer, G. S. Khakimzyanov, and N. Yu. Shokina, "Use of analytic solutions in the statement of difference boundary conditions on a movable shore line," Russ. J. Numer. Anal. Math. Model. **26**, 353–377 (2011).
16. N. M. Borisova, A. V. Gusev, and V. V. Ostapenko, "Propagation of discontinuous waves along a dry bed," Fluid Dynam. **41**, 606–618 (2006).
17. Coastal and Hydraulics Laboratory. http://chl.erdc.usace.army.mil/chl.aspx?p=s&a=Projects;35/
18. GEBCO General Bathymetric Chart of the Oceans. www.gebco.net/data_and_products/gridded_bathymetry_data/
19. Index of /srtm/version2_1/SRTM3/Eurasia. http://dds.cr.usgs.gov/srtm/version2_1/SRTM3/Eurasia/
20. C-MAP M-AN-C013.12 Kamchatka peninsula and Kuril islands.
21. E. F. Savarenskii, V. G. Tishchenko, A. E. Sviatlovskii, A. D. Dobrovolskii, and A. V. Zhivago, "Tsunami of November 4–5, 1952," Bull. Soveta Seismol. AN SSSR, No. 4, 36–37 (1958).

Translated by I. Pertsovskaya